Transport properties of organic vapours in silicone/clay nanocomposites

C. Labruyère [a], G. Gorrasi [b,*], F. Monteverde [c], M. Alexandre [d], Ph. Dubois [a,c,*]

[a] Center of Innovation and Research in Materials & Polymers (CIRMAP), Laboratory of Polymeric and Composite Materials, UMH, Place du Parc 20, B-7000 Mons, Belgium
[b] Department of Chemical and Food Engineering, University of Salerno, Via Ponte don Melillo, 84084 Fisciano, Italy
[c] Materia Nova ASBL, Avenue N. Copernic 1, B-7000 Mons, Belgium
[d] Center for Education and Research on Macromolecules (CERM), University of Liège, Building B6a, 4000 Liège, Belgium

ARTICLE INFO

ABSTRACT

Poly(dimethylsiloxane) (PDMS)/clay nanocomposites have been synthesized using a novel ω-ammonium functionalized oligo-PDMS surfactant (PDMS–$N^+(CH_3)_3$) and processed in membrane form. In order to relate the clay morphological structure to the degree of dispersion and physical properties of the membrane, the clay ion-exchanged by PDMS–$N^+(CH_3)_3$ has been compared to a non-exchanged sodium MMT and to two organoclays organo-modified by using either non-functional alkyl ammonium cations ($C_{38}H_{80}N^+$) or hydroxyalkyl ammonium ($C_{22}H_{48}ON^+$) cations. Morphological analysis and transport properties (sorption, diffusion and permeability) have been investigated using two penetrants: acetone and *n*-hexane. The mechanical and rheological properties of the PDMS nanocomposite membranes have also been studied. It has been found a significant effect of the clay organo-modifier on the morphology, physical and barrier properties of the systems.

© 2008 Elsevier Ltd. All rights reserved.

1. Introduction

Polysiloxanes and particularly poly(dimethylsiloxane) (PDMS), are very interesting materials used in a large variety of applications such as electronics, building materials or biomedical developments thanks to their exceptional properties such as electrical insulation, thermal resistance, sealing ability, good stability to weathering and biocompatibility. PDMS is also well known as a polymer very permeable to gases and vapours because of large free volume appearing between the macromolecular chains as a result of the high flexibility of the siloxane bond. This property is largely used in many industrial applications, e.g., in solvent recovery systems using separation membranes [1], in O_2 enrichment of air systems [2], or in packaging, e.g., to ensure an efficient breathing of vegetables through protective film [3]. Nevertheless, in many specific cases this high permeability of PDMS film coatings is a drawback and exchanges of gases must be avoided. Indeed, some supplies as meat or potato chips have to be protected against atmospheric gases and sparkling soda must conserve a certain concentration of gas until the sale to guarantee a good preservation and aspect. In the field of construction, an effective protection of the walls against moisture propagation by permeation is also required to preserve the thermal insulation.

Several methods can tune the permeability of silicone membranes. For example, a reduced O_2 permeation was observed [4,5] by plasma treatments of silicone membranes leading to the formation of an impermeable thin oxidized siloxane surface $(Si–O)_x$. By changing the nature of the chemical groups grafted to silicon atom, the membrane behaviour can also be modified for several vapours [2] but generally many other properties such as mechanical characteristics, thermal stability, reactivity, polarity are consequently modified. Nevertheless, an easier and more adapted solution to industrial processing consists in introducing impermeable inorganic nanometric fillers. As predicted by models [6] and already reported in studies concerning various polymer matrices [7,8], delaminated clay nanoplatelets are inorganic fillers of choice to induce barrier properties at rather low content due to their high aspect ratio. Indeed, they impede the gases to directly cross the material and induce a longer diffusion pathway due to a more tortuous gas path. Nevertheless, these hydrophilic materials do not generally delaminate when incorporated in a hydrophobic polymer and keep their original micrometric stacked structure. Accordingly, many studies have concerned methods allowing the efficient dispersion (individualization) of clay nanolayers in the polymer matrix so as to produce high performance polymer nanocomposites. Among them, several publications [9–13] report on the preparation of PDMS/clay composites using specific compatibilizers or techniques of dispersion to reach efficient delamination but few deal with the barrier properties of resulting materials and the structure/permeability relationships characterizing these compositions. Among these works, one can

* Corresponding authors.
E-mail addresses: ggorrasi@unisa.it (G. Gorrasi), philippe.dubois@umh.ac.be (Ph. Dubois).

quote Lebrun et al. [14] that incorporated layered $HTiNbO_5$ in room temperature vulcanised (RTV) PDMS resins, reaching a disordered intercalated morphology, leading to permeation to small gases (N_2, O_2, CO_2, CH_4 and C_2H_4) that proved to drop down by about 30% only at high nanofiller loading (>10 wt%). More recently, Vaughan et al. [15] observed a reduction of about 10% of permeation to small gases (N_2, O_2, CO_2, CH_4 and He) by incorporating 5 wt% of intercalated layered aluminophosphate $[Al_3P_4O_{16}]^{3+}\cdot 3[NH_3CH_2CH_3]^+$. Finally, Liu et al. [16] reported on an intercalated/exfoliated structure using a commercial organo-modified clay, i.e., Cloisite® 30B (5 wt%), leading to a reduction of 19% of the diffusion coefficient of dichloromethane vapours through RTV silicone membranes. These studies only focused on RTV silicone resins, however there are also huge interests for the exfoliation of clay in PDMS resins cross-linked by hydrosilylation (HTV PDMS) since this particular silicon resin is largely investigated in many different industrial fields [17].

This paper reports on the production and characterization of PDMS nanocomposites cured by hydrosilylation and filled with montmorillonite ion-exchanged with a newly synthesized ω-ammonium functionalized poly(dimethylsiloxane) oligomer ($PDMS-N^+(CH_3)_3$) [18]. The so-produced nanocomposites were characterized by a good extent of delamination and were compared with either unfilled PDMS or PDMS resin filled with more conventional (organo)clays characterized by different states of filler dispersion in order to correlate the composition morphological (nano)structure to the mechanical and transport properties of the recovered materials. A series of nanocompositions was further prepared by filling the PDMS resin with various $PDMS-N^+(CH_3)_3$-modified clay contents in order to evaluate the influence of the layered silicate fraction on the transport properties. The dispersion state of the different (organo)clays was determined by transmission electron microscopy (TEM) while the evolution of the viscosity, mechanical and swelling properties were investigated. Interestingly, transport properties through unfilled PDMS and PDMS (nano)-composites were determined by microgravimetric analysis using acetone and n-hexane as permeants and allowing to extract information on sorption (S), diffusion (D) and permeability ($P = S\cdot D$) at different vapour pressures. Acetone and n-hexane have been selected because they are characterized by different dimensions, solubility parameters, and degrees of interaction with PDMS resins and/or (organo)clays, and therefore can give useful information on the role played by the presence of the impermeable layered silicates and the extent of their dispersion within the cured silicone materials.

2. Experimental

2.1. Materials

HTV PDMS two-component resin used in this work was Sylgard 184 from Dow Corning. Cloisite® Na^+ is a purified sodium montmorillonite (MMT) with a cationic exchange capacity (CEC) of 92.6 meq/100 g supplied by Southern Clay Products (USA). Dimethyldioctadecyl ammonium bromide ($C_{38}H_{80}NBr$) was supplied by Acros. Tetrabutylammonium hexachloroplatinate(IV), dimethylethanolamine, 1-bromooctadecane and acetone were purchased from Aldrich. All chemicals were used as received.

2.2. Preparation of surfactants

$PDMS-N^+(CH_3)_3Br^-$ with $\overline{M}_n$ evaluated by ^{1}H NMR as 1,400 g/mol was obtained as previously described [18]. Hydroxy-ethyldimethyloctadecylammonium bromide ($C_{22}H_{48}ON^+.Br^-$) was synthesized from dimethylethanolamine and 1-bromooctadecane (10 eq mol) in ethanol during 18 h at 70 °C, precipitated in ether and dried for 16 h at 80 °C under reduced pressure. ^{1}H NMR spectrum showed that the reaction was complete (ppm, CDCl3): 0.88 (t, 3H), 1.25 (m, 30H), 1.75 (m, 2H), 3.37 (s, 6H), 3.52 (t, 2H), 3.75 (t, 2H), 4.15 (m, 2H).

2.3. Preparation of organoclay

The preparation of the organoclays containing $C_{38}H_{80}N^+$ or $PDMS-N^+(CH_3)_3$ was carried out as described elsewhere [18]. The unmodified clay (MMT/Na^+) was obtained by swelling Cloisite® Na^+ in deionised water for 16 h at 80 °C then the slurry was concentrated by centrifugation at 4,000 rpm for 10 minutes. The clay modified with $C_{22}H_{48}ON^+$ was prepared in a very similar way: Cloisite® Na^+ (10 g) and $C_{22}H_{48}ON^+.Br^-$ (1.2 eq N^+ related to CEC of clay) were separately dispersed in respectively 900 ml and 100 ml of deionised water for 3 h at 70 °C before mixing both solutions for 16 h at 80 °C. Then, the resulting organoclay suspension was filtrated and washed with deionised water at 80 °C until no more AgBr formed in supernatant following addition of AgNO3. The organoclays were kept wet (min. 75 wt% water) and the degree of organomodification was estimated by thermogravimetric analysis (TGA). Table 1 presents the composition of the (organo)clay samples used in this work.

2.4. Nanocomposite preparation

In order to prepare the PDMS/clay composites, wet (organo)-clays were dispersed in THF using ultra-sonication (with a 130 W probe: diameter = 13 mm) for 10 min in the presence of an acetone solution of tetrabutylammonium hexachloroplatinate(IV) as additional hydrosilylation catalyst in specific proportions (except for unfilled and MMT/Na^+ filled resin), then Sylgard 184 liquid resin (Part A) was added and dispersed for additional 10 minutes. The used proportions were: 1 ml THF/g final composite; 0.5 mg tetrabutylammonium hexachloroplatinate(IV)/g Sylgard 184 Part A; 0.15 ml acetone/mg tetrabutylammonium hexachloroplatinate(IV). Solvents were evaporated under reduced pressure for 16 h at 80 °C. Vulcanisation occurred, after addition of the curing agent of Sylgard 184 (Part B), at 105 °C in a 500 μm (or more) depth mould for minimum 4 h. In this work, the inorganic filler content (expressed in wt%) is given on the basis of the clay/PDMS uncured dispersions before their cross-linking. The sample codification is reported Table 2.

Table 1
(Organo)clay composition.

	Organic surfactant content in dried organoclay (wt%).
MMT/Na^+	0
$MMT/C_{38}H_{80}N^+$	44
$MMT/C_{22}H_{48}ON^+$	28
$MMT/PDMS-N^+(CH_3)_3$	50

Table 2
Sample compositions and codes.

Sample code	wt% filler in uncured resin	Clay filler code
PDMS	0	No filler
3MMT	3	MMT/Na^+
3MMT–Alkyl	3	$MMT/C_{38}H_{80}N^+$
3MMT–AlkylOH	3	$MMT/C_{22}H_{48}ON^+$
1MMT–PDMS	1	$MMT/PDMS-N^+(CH_3)_3$
2MMT–PDMS	2	$MMT/PDMS-N^+(CH_3)_3$
3MMT–PDMS	3	$MMT/PDMS-N^+(CH_3)_3$
4MMT–PDMS	4	$MMT/PDMS-N^+(CH_3)_3$
5MMT–PDMS	5	$MMT/PDMS-N^+(CH_3)_3$
6MMT–PDMS	6	$MMT/PDMS-N^+(CH_3)_3$

Fig. 1. Chemical structure of PDMS–N$^+$(CH$_3$)$_3$.Br$^-$.

2.5. Mechanical and morphological characterizations

^{1}H NMR analyses were carried out in CDCl$_3$ at 300 MHz and 7 T using a Bruker AMX spectrometer. Thermogravimetric analyses (TGA) were performed under He at 20 °C/min using a Q50 thermogravimetric analyzer (TA Instruments). Weight fractions of water and surfactant were estimated between room temperature and 150 °C and between 150 and 550 °C, respectively. Wide angle X-ray scattering (WAXS) analysis was carried out using a Siemens D5000 diffractometer in reflectance mode with the Cu Kα radiation (λ = 0.15406 nm) from 1.5 to 22° by step of 0.04° each 2 seconds and the generator voltage and current were 40 kV and 40 mA, respectively. Transmission electron microscopy (TEM) micrographs were obtained with a Philips CM100 apparatus using an acceleration voltage of 100 kV. Ultrathin sections of the composites (c.a. 80 nm thick) were cut at −100 °C from the cured samples with a LEICA ultra-cryomicrotome equipped with a diamond knife. The viscosity of PDMS and PDMS/clay suspension was determined using a Brookfield viscometer equipped with cone/plate geometry (diameter: 24 mm; angle: 3°) at 4 rpm and 25 °C. The maximum standard deviation for these viscosity results was 2%. The swelling rate was determined by measuring the increase of weight at steady state of cured PDMS samples placed in n-heptane normalized with the weight of the dried samples after analysis. In every case (unfilled matrix and composites), the amount of extractible materials was around 5 wt% of the initial sample. Stress–strain curves were obtained using a dynamic mechanical thermo-analyzer (DMTA 2980 from TA Instruments) in tensile mode at 29 °C with 1 Hz oscillations through increasing step-by-step deformation until a strain of 0.3%. The density of the PDMS membranes (ρ) was calculated following a procedure proposed by the balance supplier Ohaus (using Archimedes method) and based on measurement of their weight in water.

2.6. Transport properties

Transport properties experiments were performed using a conventional McBain spring balance system, which consists of a glass water-jacketed chamber serviced by a high vacuum line for sample degassing and permeant removal [19]. Inside the chamber samples were suspended from a helical quartz spring supplied by Ruska Industries, Inc. (Houston, TX) and had a spring constant of 1.892 cm/mg. The temperature was controlled to 30 ± 0.1 °C by a constant temperature water bath. Before beginning the sorption experiments, the sample was exposed to vacuum for at least 24 h in order to remove previously sorbed air gas and water vapour from the polymer. Permeants used were acetone (solubility parameter: 9.90 (cal/cm^3)$^{1/2}$) and n-hexane (solubility parameter: 7.30 (cal/cm^3)$^{1/2}$) [20]. Sorption was measured as a function of the relative pressure, a = P/P$_0$, where P is the actual pressure (in mmHg) of the experiment, and P$_0$ the saturation pressure at 30 °C for acetone (273 mmHg) and n-hexane (200 mmHg). The samples were exposed to the penetrants at fixed pressures, and the spring position was recorded as a function of time using a cathetometer. The spring position data were converted to mass uptake data using the spring constant. Diffusion coefficients and equilibrium mass uptake were extracted from these kinetic sorption data.

3. Results and discussion

Several studies on PDMS/clay composites showed the importance to reduce the hydrophilicity of the clay surface to obtain an efficient dispersion of delaminated clay and to promote attractive interactions between the hydrophobic polymer matrix and the mineral phase. Recently [18], we reported on the preparation and the characterization of intercalated/exfoliated nanocomposites based on montmorillonite and HTV PDMS resin. These nanocomposites were obtained owing to the simultaneous use of a novel ω-ammonium functionalized oligo-PDMS surfactant of 1,400 g/mol (PDMS–N$^+$(CH$_3$)$_3$) (Fig. 1) and a new dispersion procedure using aqueous THF solution and ultra-sonication (see experimental section). The same procedure was used in this study. So, all the
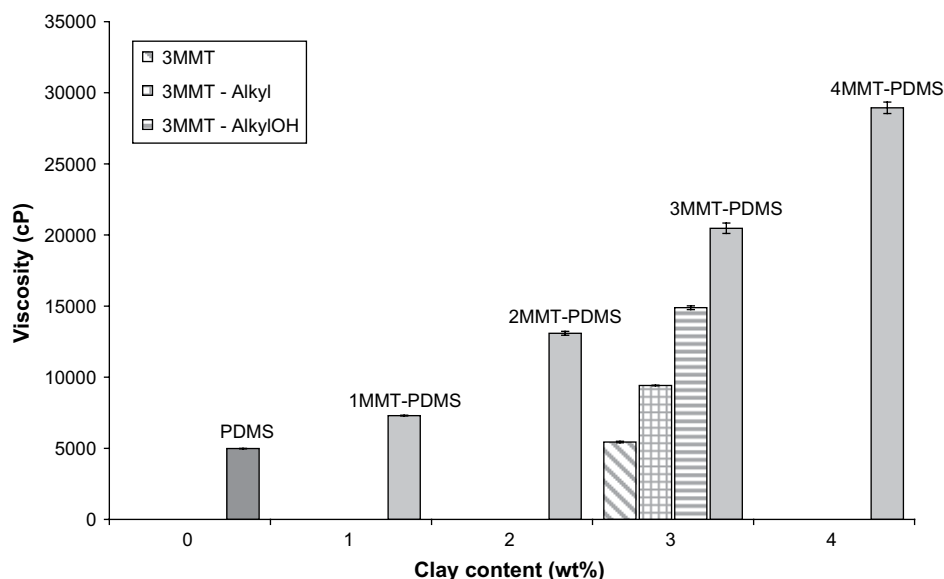
Fig. 2. Viscosity of PDMS/clay dispersion containing different organoclays (at 3 wt%) and at different clay contents for the nanocomposites containing the PDMS–N$^+$(CH$_3$)$_3$ surfactant.
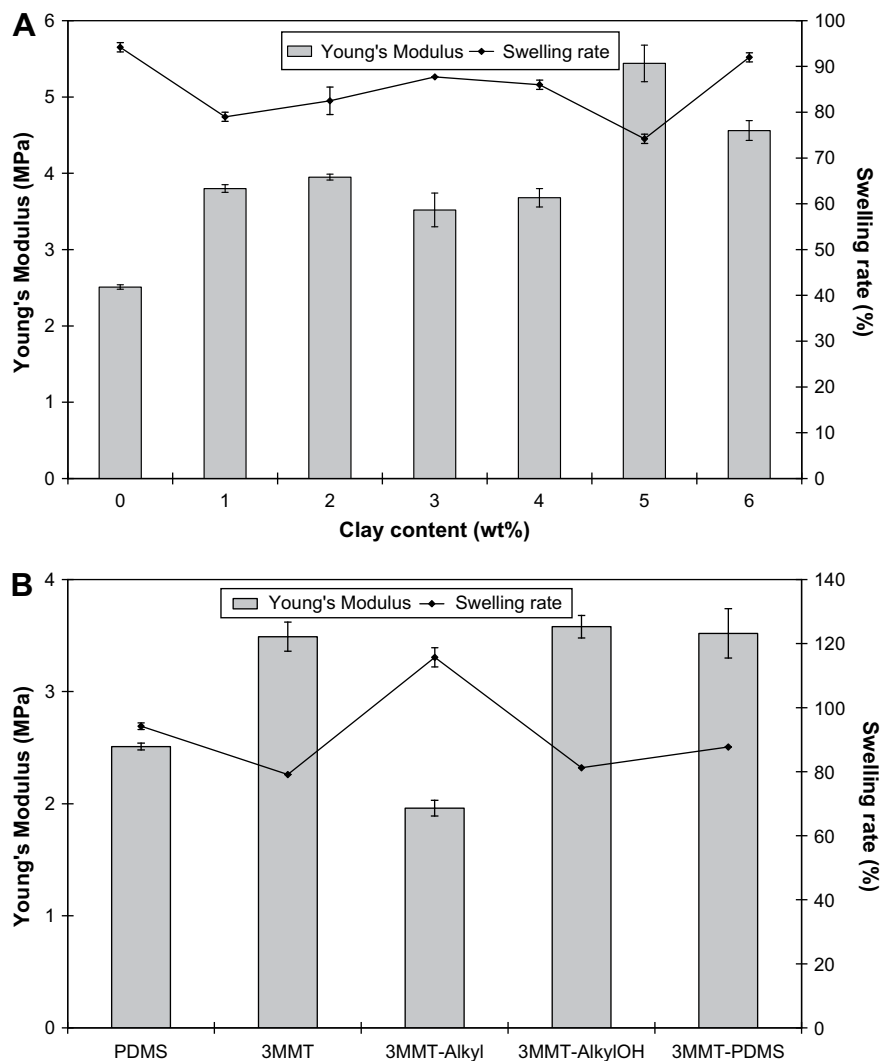
Fig. 3. Swelling rate and Young's modulus of composites containing increasing contents of MMT/PDMS–N$^+$(CH$_3$)$_3$ (A) and the different (organo)clays (B) (unfilled cured PDMS is also presented for sake of comparison).

organoclays have been first surface-exchanged before being dispersed in the resin. In order to relate the clay morphological structure to the permeability of the membrane, the promising clay ion-exchanged by PDMS–N$^+$(CH$_3$)$_3$ has been compared to a non-exchanged sodium MMT and to two organo-modified clays. These last ones have been organo-modified by using non-functional alkyl ammonium cations (C$_{38}$H$_{80}$N$^+$) or by using hydroxyalkyl ammonium (C$_{22}$H$_{48}$ON$^+$) cations, given rise to organoclay exchanged with oniums analogous to widely used commercial Cloisite$^\circledR$ 20A and Cloisite$^\circledR$ 30B, respectively. Moreover, various inorganic contents of MMT/PDMS–N$^+$(CH$_3$)$_3$ were introduced in the PDMS resin to determine the influence of the inorganic proportion on the transport properties. The different materials samples prepared in this study are shown in Table 2.

Several methods of characterization have been investigated to assess for the clay nanoplatelet dispersion by giving direct information concerning the dispersion of the platelets, i.e., transmission electron microscopy (TEM) and wide angle X-ray diffraction (WAXD) analyses as performed on cross-linked composites. Indirect information was also obtained by measuring the viscosity of the uncured composite and evaluating the swelling rate and the stiffness of the cross-linked composites.

3.1. Viscosity

Rheological properties of PDMS/organoclay nanocomposites offer convenient insight into their microstructure and are generally measured to attest for the extent of dispersion of clay platelets [21]. Actually, the rheological response, e.g., shear viscosity of melt clay-filled polymer, arises mainly from frictional interactions between the silicate layers and to a lesser extent from attractive interactions establishing between polymer and particles [22]. With improving the exfoliation of layers and increasing the clay content, these interactions become stronger and more numerous leading to higher values of viscosity.

The neat uncured matrix shows a viscosity of 5,000 cP (or mPa·s). At 3 wt% of inorganic content, significant differences are found between composites containing the four types of clay (Fig. 2). A very slight increase in viscosity (5,500 cP) is observed as a non-treated MMT/Na$^+$ is incorporated in PDMS (3MMT) indicating that an organic surfactant is needed to intercalate this filler and to interact with the host polymer. In the PDMS/organoclay suspensions, the presence of alkyl ammonium (C$_{38}$H$_{80}$N$^+$) and hydroxy-lalkylammonium (C$_{22}$H$_{48}$ON$^+$) cations leads to higher viscosities (9,400 and 15,000 cP). As aforementioned, these higher values
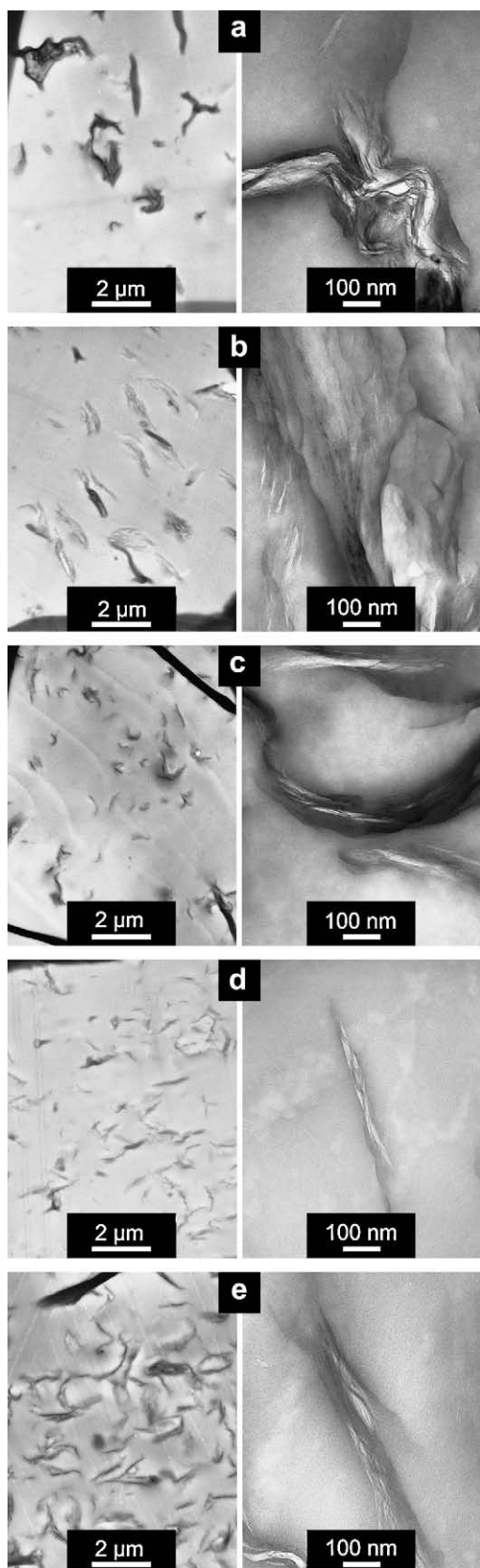
Fig. 4. TEM micrographs of cured PDMS (nano)composites: (a) 3MMT, (b) 3MMT–Alkyl, (c) 3MMT–AlkylOH, (d) 3MMT–PDMS and (e) 6 MMT–PDMS (see Table 2).

attest for the usefulness of the alkyl cation in the intercalation of the resin and for the favourable interactions such as van der Waals and H-bonding (only for the hydroxyl-containing surfactant) established between the organoclay and the matrix. However, significantly more important viscosity (20,500 cP) was obtained with PDMS–$N^+(CH_3)_3$ surfactant. This silicone oligomer renders the penetration of the matrix in the clay gallery more efficient leading to a larger delamination of the clay stacks and platelets and promotes favourable chemical interactions between this organoclay and the matrix.

The clay content of the nanocomposites containing the PDMS–$N^+(CH_3)_3$ surfactant was varied from 1 to 6 wt%. It was observed that the viscosity increases constantly with the clay content up to about 29,000 cP at 4 wt%, which represents almost a six-fold increase of the viscosity with respect to the pristine silicone oil. The growth of viscosity seems constant indicating that nanoplatelets or small stacks have enough space to disperse and no agglomeration appears. It is worth pointing out that the viscosity of compositions containing more than 4 wt% was too high to be measured with the used viscometry apparatus.

3.2. Mechanical properties

To promote hydrosilylation reaction of the nanocomposites containing ammonium surfactants, tetrabutylammonium hexachloroplatinate(IV) (500 ppm) was required as an additional catalyst. Indeed, it was not possible to cure the composites containing ammonium surfactants simply by adding the curing agent present into the Sylgard 184 two-component composition. This poisoning effect on H_2PtCl_6 catalyst was already reported by Sabourault et al. [23] who attributed it to the ammonium/(remaining free) amine functions. Hydrosilylation was therefore promoted by adding tetrabutylammonium hexachloroplatinate(IV). In spite of the additional catalyst, the clay modified with the alkyl ammonium cation ($MMT/C_{38}H_{80}N^+$) still poisons the curing reaction leading to lower Young's modulus and higher swelling rate of the composite sample in comparison to the unfilled cured resin (Fig. 3B).

In the other compositions, the presence of (organo)clays increases the apparent degree of cross-linking as shown by the reduced swelling rate in *n*-heptane (Fig. 3A and B). The swelling results obtained from composites containing 3 wt% of different organoclays are however similar while the increase in the mechanical properties is far less important than expected from such compositions. As far as the effect of MMT–PDMS content is concerned, there is apparently no direct relation between the stiffness and clay content even if, at higher filler loadings, resulting nanocomposites exhibit higher Young's modulus values. These mechanical performances can be explained by the inherent presence, within the Sylgard 184 composition, of micro-networks of siloxane covalently bonded to the elastomer. These highly functional micro-networks, present in significant proportion (30 wt%), hide any stiffening effect that would result from the presence of clay nanoplatelets. But this limited stiffness increase could also have another origin. Indeed, to date, even if polysiloxane-based surfactants has been rarely considered for organo-modifying MMT, the reported works attest for limited mechanical enhancement more likely due to a rather poor quality of clay delamination, i.e., mostly intercalation took place in the cured silicone matrix [13,14]. These observations lead to think that PDMS chains could not be the more adapted surfactants to promote good adhesion between clay and PDMS matrix. Actually, PDMS chains present a rather low density of cohesive energy. So they could be efficient to intercalate siloxane macromolecule in clay gallery but they establish weak intermolecular forces within the host matrix.

3.3. Morphology

TEM pictures of (nano)composites based on non-treated MMT and the organo-modified clays (Fig. 4a–e, systematically recorded at two observation scales) give information in agreement with the viscosity measurements. The quality of dispersion of the four different clays is gradually enhanced using compatibilizers promoting attractive interactions with the matrix. Micrometric aggregates are observed in composites based on sodium MMT

(3MMT) (Fig. 4a). Organoclays containing respectively alkyl ammonium ($C_{38}H_{80}N^{+}$) or hydroxylalkylammonium ($C_{22}H_{48}ON^{+}$) surfactants tend to form stacks with thickness respectively of about 300–500 and 100–200 nm revealing a low but increased degree of dispersion (3MMT–Alkyl, 3MMT–AlkylOH) (Fig. 4b and c). In contrast, the nanocomposite based on MMT/PDMS–$N^{+}(CH_3)_3$ (3MMT–PDMS) (Fig. 4d) exhibits a homogeneous distribution of ca. 50 nm-thick and 1 μm-long stacks of a few tens nanoplatelets revealing a significantly higher degree of dispersion. This new
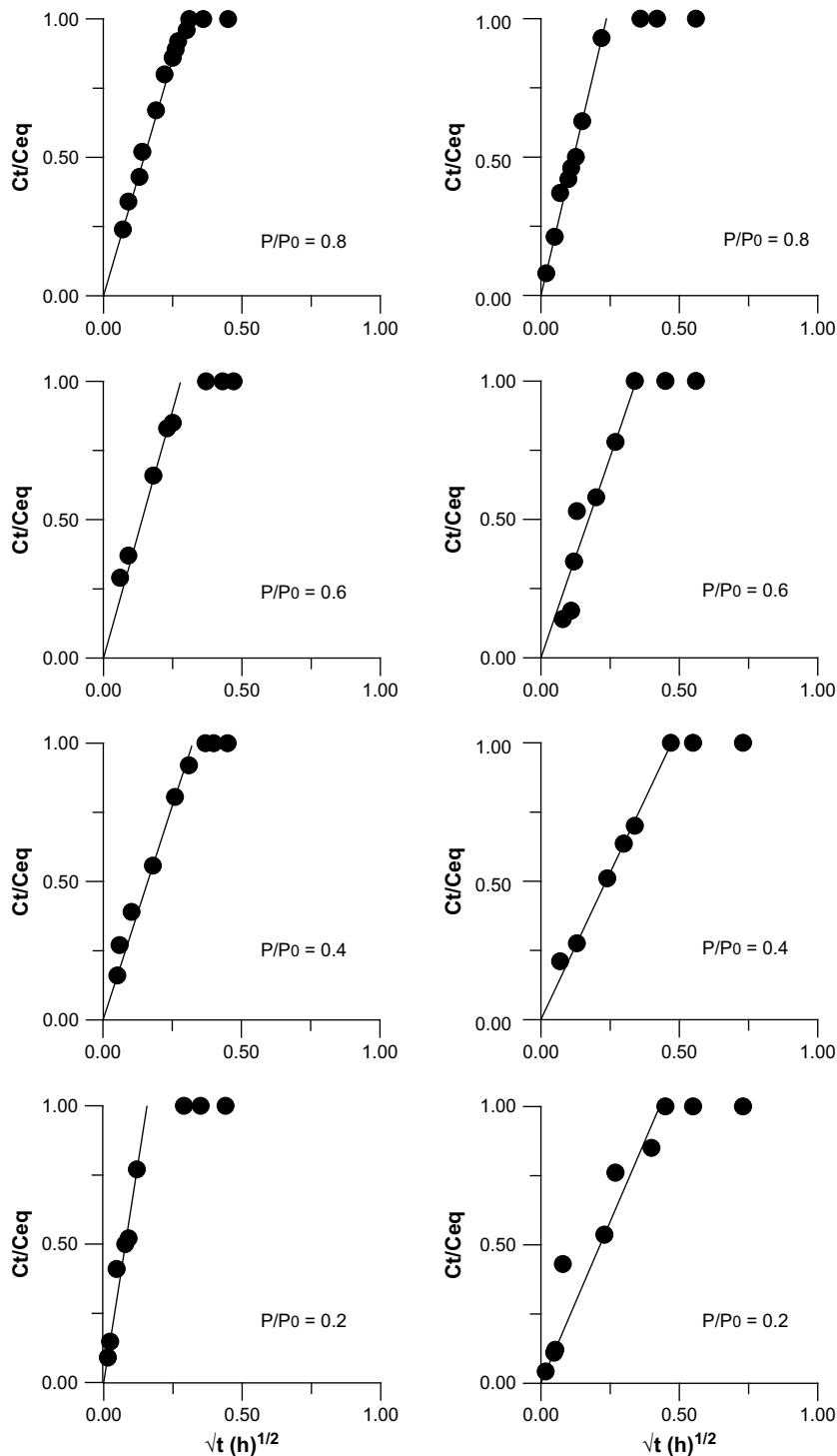

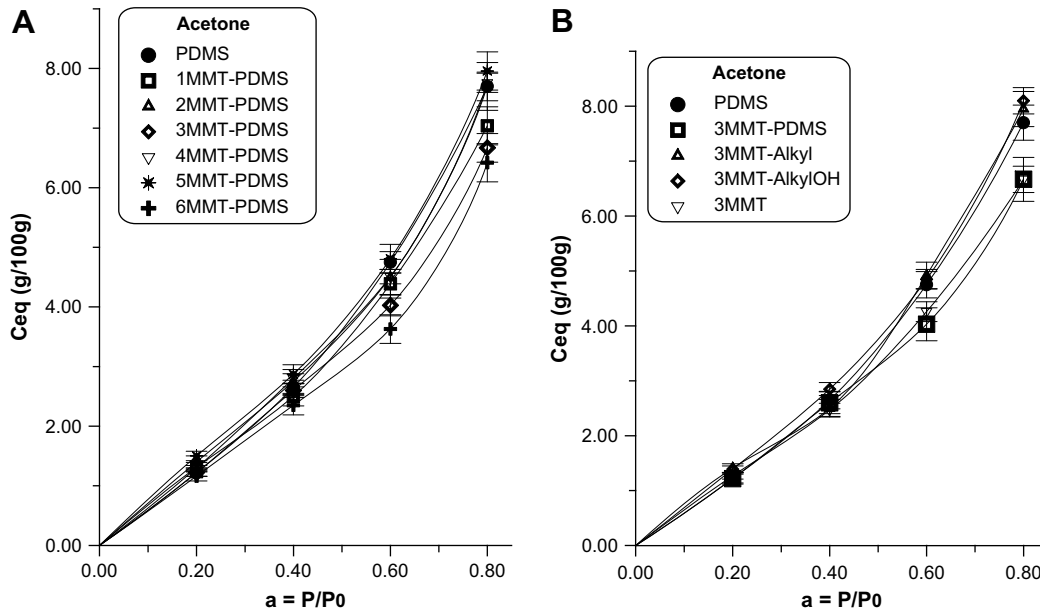**Fig. 5.** Acetone sorption kinetics for PDMS (left) and for 3MMT–PDMS (right).

Fig. 6. Acetone sorption isotherms of unfilled PDMS and related (nano)composites filled with different (organo)clays.

silicone surfactant combined with use of water/THF solution as a dispersive medium, used to incorporate the clay into the matrix allows reaching an under-micrometric breakdown of clay stacks never seen before in hydrosilylated HTV PDMS. When increasing the clay content from 3 to 6 wt% (Fig. 4d and e), the thickness of clay stacks slightly increases (around 200 nm) but no micrometric-thick aggregates can be observed and the good distribution is preserved throughout the matrix. In each picture, one can observe that clays are randomly distributed and do not present any preferential orientation. It is worth noting that the composite samples were not prepared following a process that favours the orientation of the clay platelets. Indeed, there are at least two orders of magnitude between the maximum size of the stacks (ca. 1 μm) of clay and the thickness of the membrane (about 500 μm) that permits them to take any possible orientations.

WAXS analysis has been approached by using 500 μm-thin (nano)composite films, however the recorded diffractograms (not shown herewith) did not display any differences between unfilled PDMS and the studied (nano)composites. Whatever the investigated sample, only two broad diffraction signals centered at about 6° and 12° were observed and could be attributed to the micro-networks of siloxane contained in the pristine Sylgard 184 formulation and to the polysiloxane matrix, respectively. No diffraction peak characteristic of the organo-modified clays could be observed more likely masked by the first broad peak at ca. 6°.

3.4. Transport properties

Polymeric nanocomposites have a wide spectrum of relaxation times associated with the motion of the polymer segments in confined environments. An increase of either temperature or concentration of the permeant in the polymer leads to a decrease of the relaxation times, and thus to an enhanced motion of the polymer segments. The diffusion of small molecules through polymeric nanocomposites is associated with the finite rates at which the polymer structure changes in response to the motion of the permeant molecules and the degree of dispersion of the clay platelets. Solubility and diffusivity can be further modified by the presence of inorganic fillers and molecular orientation. More particularly, inorganic fillers are believed to increase the barrier
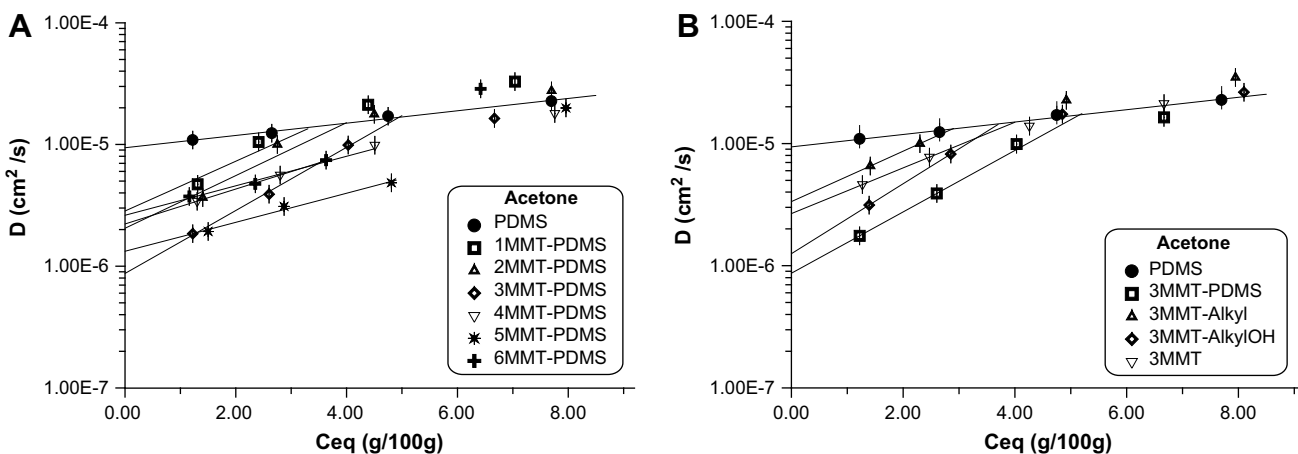

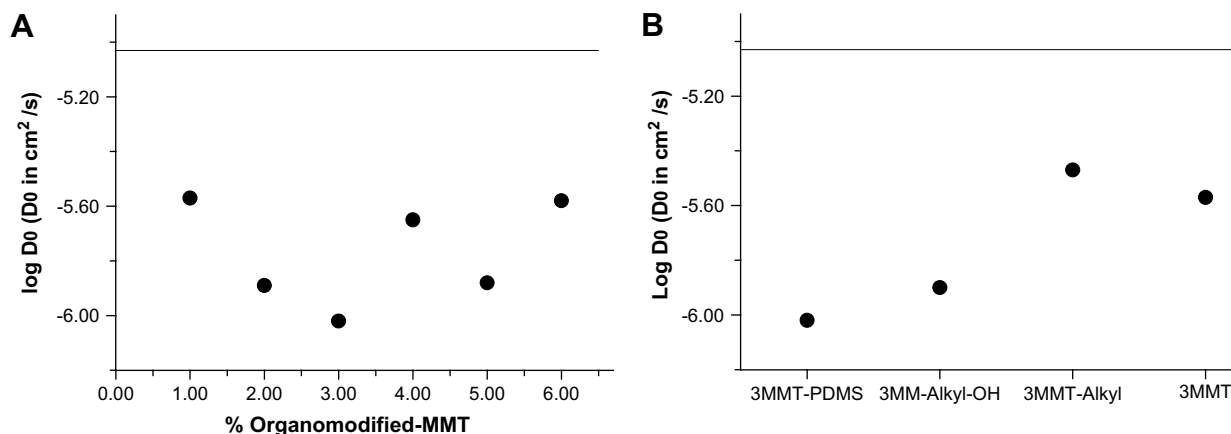**Fig. 7.** Acetone diffusion parameter of unfilled PDMS and related (nano)composites filled with different clays.

Fig. 8. Values of logarithm of the zero diffusion coefficient (Log D_0) of composites filled with different (organo)clays evaluated with acetone (upper straight line corresponds to unfilled PDMS).

properties by creating a maze or "tortuous path" that retards the progress of the small molecules through the polymeric matrix. The direct benefit of the formation of such a path is clearly observed in all the prepared nanocomposites by dramatically improved barrier properties [24].

There is also evidence that the nano-sized clay restricts the molecular dynamics of the polymer chains surrounding the clay, thus retarding the relaxation of polymer chains. The retarded relaxation, in turn, reduces the diffusion of small molecules through the nanocomposites [25].

Therefore, to determine how the content and the chemical modification of layered silicate in the PDMS/clay (nano)composites affects the permeability, the transport properties were measured for all the samples using acetone and *n*-hexane vapours. The use of two solvents, having different dimensions, solubility parameters, and different degrees of interaction with the polymer matrix, can give useful information on the amorphous phases in the presence of the impermeable layered silicate. It is worth pointing out that water vapour was initially considered but since no significant weight uptake could be recorded for unfilled PDMS samples, this permeant was not further investigated.

3.4.1. Acetone vapour

Measuring the increase of weight with time, for the samples exposed to the vapour at a given partial pressure, it is possible to obtain the equilibrium value of sorbed vapour, C_{eq} ($g_{solvent}$/100 $g_{polymer}$). Moreover, in the case of Fickian behaviour, that is a linear dependence of sorption on square root of time, it is possible to derive the mean diffusion coefficient from the linear part of the reduced sorption curve, reported as C_t/C_{eq} versus square root of time, by the Eq. (1) [26]

$$\frac{C_t}{C_{eq}} = \frac{4}{d}\left(\frac{Dt}{\pi}\right)^{1/2} \tag{1}$$

where C_t is the penetrant concentration at the time t, C_{eq} is the equilibrium value, and d in cm is the thickness of the sample. All the samples showed a Fickian behaviour during the sorption of acetone vapour at different activities. Fig. 5 reports the sorption kinetic curves (C_t/C_{eq} vs. square root of time) for the samples PDMS (Fig. 5 (left)) and the 3MMT–PDMS (Fig. 5 (right)) as representative of all the samples.

Using Eq. (1) it was possible to derive the average diffusion coefficient, D (cm²/s), at every fixed vapour activity ($a = P/P_0$).

The solubility coefficient, S, in cm³(STP)/(cm³.atm), can be calculated from C_{eq} as follows:

$$S = \frac{C_{eq}}{100}\frac{\rho}{MW_{penetrant}}\frac{22,414}{P} \tag{2}$$

Where ρ is the sample density, P is the penetrant pressure in atm, $MW_{penetrant}$ is the penetrant molecular weight in g/mol, and 22,414 is a conversion factor.

Diffusion depends on concentration for many polymer-solvent systems, and generally this dependence can be expressed by the following empirical law [27]:

$$D = D_0 \exp(\gamma C_{eq}) \tag{3}$$

where D_0 is the thermodynamic zero-concentration diffusion coefficient, related to the fractional free volume and to the microstructure of the polymer; γ is the concentration coefficient, which depends on the fractional free volume, too, and on the plasticizing effectiveness of the penetrant.

The permeability of the samples to the vapour is given by the product of sorption and diffusion:

$$P = S \cdot D \tag{4}$$

Fig. 6 reports the acetone sorption isotherms, C_{eq} ($g_{solvent}$/100 $g_{polymer}$) as function of vapour activity for the nanocomposites with MMT organo-modified modified with PDMS–N⁺(CH₃)₃ at different percentages (A) and nanocomposites with 3 wt% of the different investigated organo-modifiers (B).

At low vapour activity the isotherms of the samples are linear, following the Henry's law, whereas exponential increase is observed at higher activities ($a > 0.4$), indicating a Flory–Huggins behaviour [27]. This behaviour represents a preference for the formation of penetrant–penetrant pairs, so the solubility coefficient continuously increases with the activity, as mathematically expressed from the equation $\ln a_s = \ln \phi_s + \phi_p + \chi \cdot \phi_p$, where a_s is the solvent activity, ϕ_s is the volume fraction of solvent, ϕ_p is the volume fraction of polymer and χ is a polymer–solvent interaction

Table 3
Permeability* data at different acetone vapour pressures for all investigated samples containing 3 wt% in inorganics (and unfilled PDMS for sake of comparison).

Sample	$P (a = 0.2)$	$P (a = 0.4)$	$P (a = 0.6)$	$P (a = 0.8)$
PDMS	7.25×10^{-4}	8.92×10^{-4}	1.48×10^{-3}	2.39×10^{-3}
3MMT	3.25×10^{-4}	5.29×10^{-4}	1.10×10^{-3}	1.96×10^{-3}
3MMT–PDMS	1.25×10^{-4}	2.81×10^{-4}	7.40×10^{-4}	1.52×10^{-3}
3MMT–Alkyl	5.14×10^{-4}	6.41×10^{-4}	2.07×10^{-3}	3.85×10^{-3}
3MMT–AlkylOH	2.40×10^{-4}	6.44×10^{-4}	1.56×10^{-3}	2.94×10^{-3}

*P((cm³)/(cm³ × atm)) × (cm²/s).

parameter based on the swelling power of the solvent with respect to the polymer. The first molecules sorbed tend to locally loosen the polymer structure and make it easier for following molecules to enter. These isotherms are observed when the penetrant effectively plasticizes the polymer, being a strong solvent or swelling agent for the polymer. No significant differences in the amount of sorbed solvent are observable between the analyzed samples, especially at low vapour pressure. This means that PDMS behaves in the same way, independently of the type of filler and its percentage. Fig. 7 (A)

and (B) reports the diffusion parameter, D (cm^2/s), as a function of the concentration of sorbed acetone for all the samples.

Unfilled PDMS shows a dependence from C_{eq} (g/100 g) of acetone, according to Eq. (3) in all the sorbed concentration range. For the nanocomposites two regions of the curves are clearly recognizable: at low vapour concentration, the diffusion coefficient increases steeply and linearly with C_{eq}, whereas at high concentration (≥ 4 g/100 g) a still linear but smoother dependence is shown by all the samples. The transition is observed for concentrations of
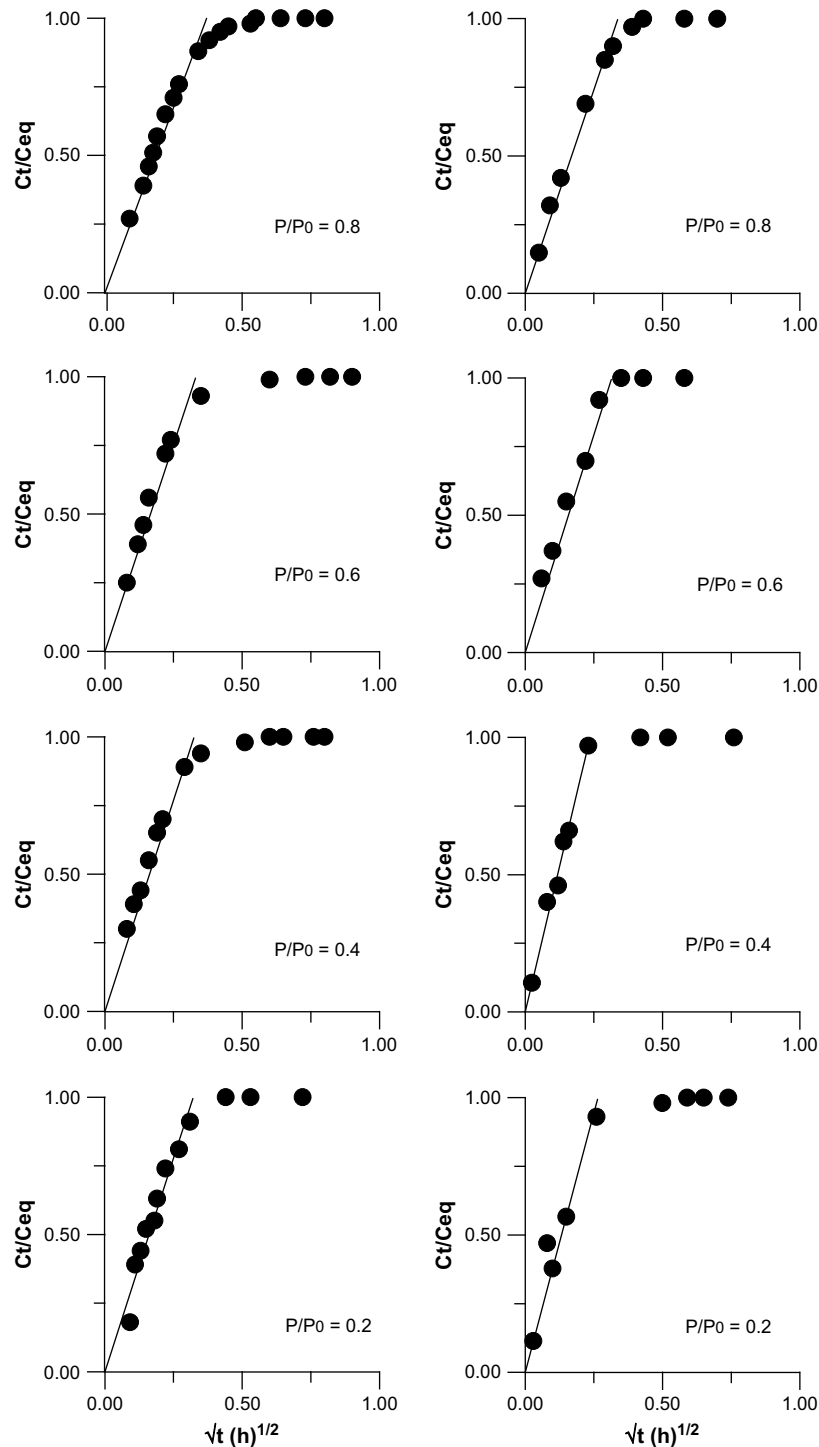

Fig. 9. (Left) n-hexane sorption kinetics for PDMS (right) n-hexane sorption kinetics for 3MMT–PDMS.
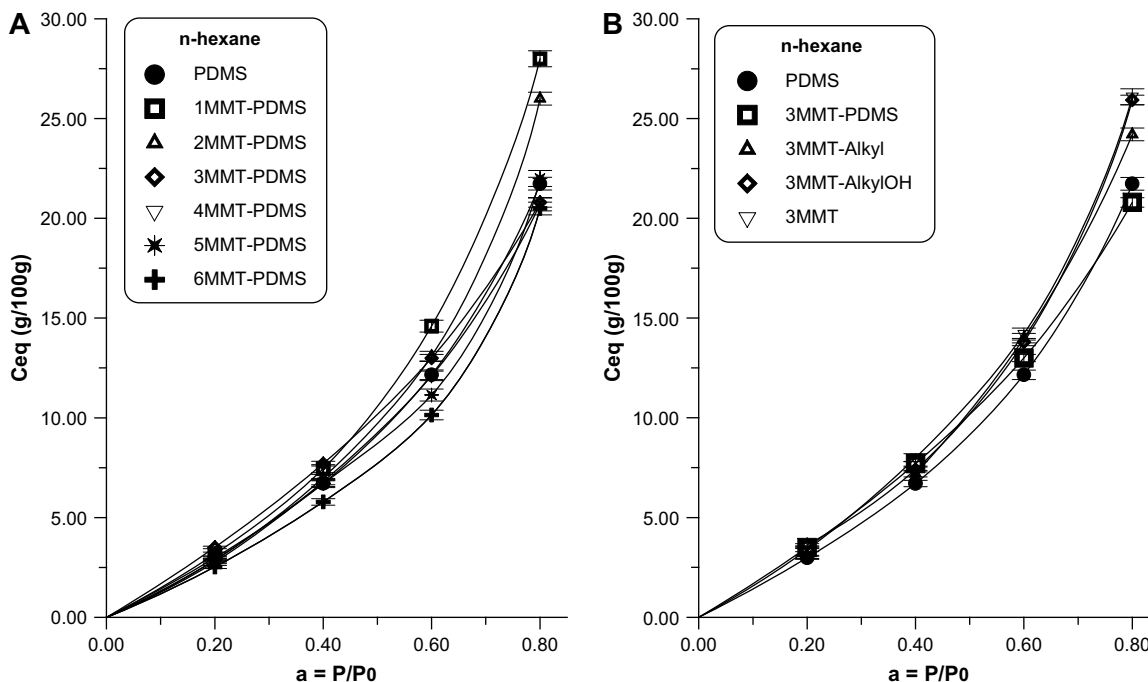
Fig. 10. *n*-Hexane sorption isotherms of unfilled PDMS and related (nano)composites filled with different clays.

sorbed vapour higher than about 3%. As we observed from the sorption curve in Fig. 7, a strong interaction was evident at high activities for amounts adsorbed higher than about 3%. The strong interaction with the penetrating molecules, leading to a high mobility of polymer chains, can induce structural transformations, as clustering of solvent molecules, crazing or partial dissolution. The systems loose their compactness and diffusion becomes less dependent or even independent of the amount of vapour adsorbed, as we can observe by the second part of the curves. From the first part of the diffusion curves in Fig. 7, we extrapolated the zero diffusion coefficient, D_0, for all the samples. Fig. 8 displays the Log D_0 (D_0 in cm^2/s) for all the analyzed samples. The horizontal straight line represents the Log D_0 of the unfilled PDMS.

All the composites show lower D_0, compared to the unfilled PDMS. There is an evident influence of the chemical modification of the MMT, its relative content and the related morphology of the

(nano)structure. The composites containing MMT as modified with PDMS–N$^+$(CH$_3$)$_3$ display a more reduced diffusion, which is proportional to the amount of filler, at least up to 3%. Within this range of composition, the tortuosity of the diffusing pathway appears increased with increasing the MMT content. However, upon further increasing the clay content, i.e., above 3%, the filler dispersion appears less efficient as observed on Fig. 4 (compare Fig. 4d and e) and therefore results in slightly higher D_0 values. Samples filled with 3% of MMT modified with alkyl groups (3MMT–Alkyl) show a behaviour very close to the one displayed by the 3MMT sample. In these latter cases a non homogeneous texture is found by the small molecules. We can hypothesize that the amount of inorganic clay platelets and the quality of layer dispersion delay the diffusion. Sample 3MMT–AlkylOH shows a D_0 similar to that of the nanocomposite filled with 3 wt% of clay modified by PDMS–N$^+$(CH$_3$)$_3$. This means that such a modifier created links (hydrogen
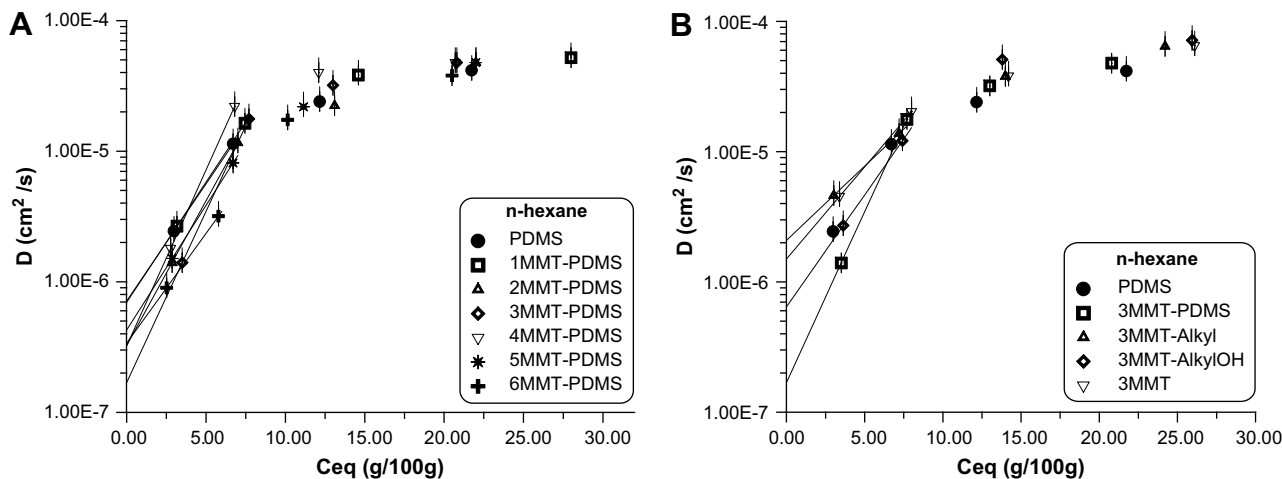

Fig. 11. N-hexane diffusion parameter of unfilled PDMS and related composites filled with different clays.
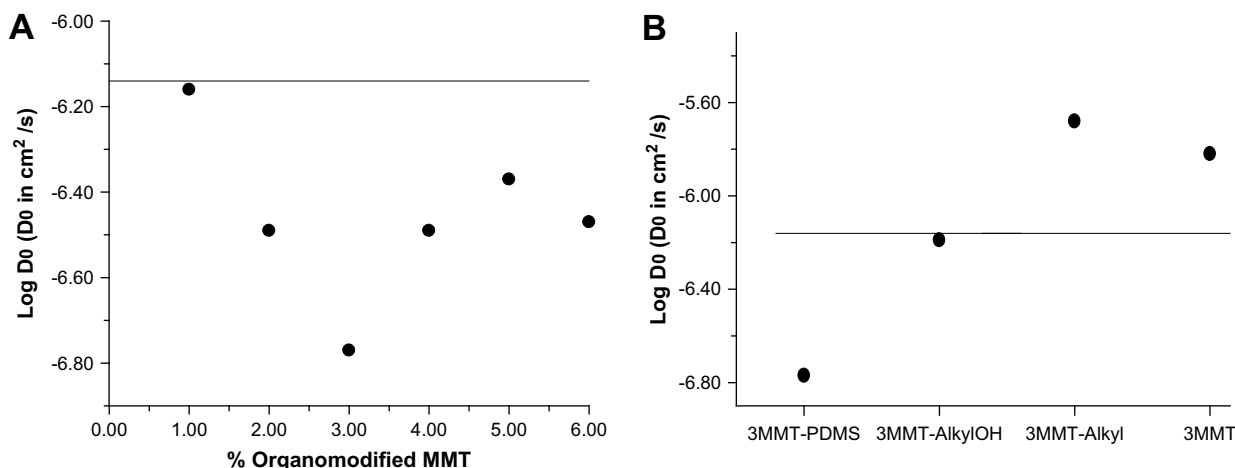
Fig. 12. Values of logarithm of the zero diffusion coefficient (Log D_0) of (nano)composites filled with different clays evaluated with n-hexane (the horizontal straight line corresponds to unfilled PDMS).

bond between hydroxyl group and oxygen atom of siloxane bonds) with the polymer matrix that can hinder the diffusion of acetone. It is worth noting that it is a thermodynamic parameter and not a technological parameter, as the diffusion coefficients evaluated at each vapour activity, which can be correlated to the use of the materials in interactive environments. D_0 values give information related to the starting structure of the samples (i.e. fractional free volume and tortuosity of the path) strictly correlated to the morphological texture.

Using Eqs. (1) and (2), for each vapour activity, we obtained sorption S $[cm^3(STP)/(cm^3.atm)]$ and diffusion D (cm^2/s), their product allowed determining the permeability. Table 3 reports the permeability data to acetone vapour pressure in the investigated range of activity (0.2–0.8) for the (nano)composite samples filled with 3 wt% in inorganics. Data for unfilled PDMS are also presented for sake of comparison.

At all vapour pressures, the introduction of unmodified clay (MMT/Na$^+$) only slightly reduces the permeation of the PDMS more likely as a result of higher sorption behaviour. Indeed even if the native montmorillonite does not finely disperse within PDMS, its polar surface can readily adsorb acetone molecules. As far as the organoclay-based composites are concerned and whatever the vapour pressure, the lowest permeation is measured for the nanocomposite containing PDMS–N$^+$(CH$_3$)$_3$ as surfactant, i.e., 3MMT–PDMS.

It is worth pointing out that transport properties in acetone of the (nano)composites cannot be differentiated from each other by taking into account their cross-linking rates since these values do not significantly differ from each other (swelling rate in acetone ranges from 22 to 26%). The morphology and the nature of organo-modifier, more than the cross-linking density, appear responsible for the improvement of the barrier properties.

3.4.2. n-hexane vapour

With the purpose to investigate the vapour transport properties of a non polar hydrocarbon solvent through PDMS and PDMS (nano)composites, n-hexane has been also considered as permeant.

Measuring the increase of weight with time, for the samples exposed to n-hexane vapour at a given partial pressure, it was possible to obtain the equilibrium value of sorbed vapour, C_{eq} (g$_{solvent}$/100 g$_{polymer}$). All the samples showed Fickian behaviour during the sorption of n-hexane vapour at different activities. Fig. (9) reports the sorption kinetic curves (C_t/C_{eq} vs. square root of time) for the samples PDMS (Fig. 9 (left)) and the 3MMT–PDMS

(Fig. 9 (right)) as representative of all the samples, so it was possible to derive the diffusion coefficient at each activity using Eq. (1).

Fig. 10 shows the sorption isotherms for the nanocomposites filled with MMT modified with PDMS–N$^+$(CH$_3$)$_3$ at different percentages (A) and nanocomposites filled with 3 wt% of different organo-modifiers (B).

Also in the presence of n-hexane vapour, the studied samples behave following the Flory–Huggins type of isotherm. The sorbed solvent values at each vapour activity are higher than the ones obtained with acetone because hexane is more interactive solvent having a solubility parameter (7.30 $(cal/cm^3)^{1/2}$) very close to the one reported for PDMS (7.58 $(cal/cm^3)^{1/2}$) [20].

No significant differences in the amount of sorbed solvent are observable between the analyzed samples, especially at low vapour pressure. The PDMS matrix behaves in the same way, independently of the type of filler and relative content. Comparing with acetone data, the higher amount of sorbed solvent in all investigated activity ranges results from the much better interaction of n-hexane with the PDMS chains. As expected, especially at higher vapour activity (i.e., 0.8), the PDMS modifier increased the equilibrium value of solvent sorbed. Fig. 11 reports the diffusion coefficients, D (cm^2/s), as a function of the C_{eq} (g/100 g) of n-hexane for the nanocomposites filled with MMT modified with PDMS–N$^+$(CH$_3$)$_3$ at different percentages (A) and nanocomposites with 3 wt% of different organo-modifiers (B).

It is evident that all the samples show two regions: at low vapour concentration, the diffusion coefficient increases steeply and linearly with C_{eq}, whereas at high concentration (≥ 7 g/100 g) a still linear dependence is shown by all the samples reaching a downward trend. The transition is observed for concentrations of sorbed vapour higher than about 7%. As underlined observing Fig. 11, a very strong interaction was evident at high activities for

Table 4

Permeability* data at different n-hexane vapour pressures for all investigated samples containing 3 wt% in inorganics (and unfilled PDMS for sake of comparison).

Sample	P ($a = 0.2$)	P ($a = 0.4$)	P ($a = 0.6$)	P ($a = 0.8$)
PDMS	3.69×10^{-4}	1.96×10^{-3}	4.97×10^{-3}	1.16×10^{-2}
3MMT-PDMS	2.48×10^{-4}	3.49×10^{-3}	7.08×10^{-3}	1.27×10^{-2}
3MMT–Alkyl	7.07×10^{-4}	2.54×10^{-3}	9.01×10^{-3}	2.00×10^{-2}
3MMT–AlkylOH	5.00×10^{-4}	2.29×10^{-3}	1.19×10^{-2}	2.38×10^{-2}
3MMT	7.79×10^{-4}	4.16×10^{-3}	9.21×10^{-3}	2.17×10^{-2}

*P$((cm^3)/(cm^3 \times atm)) \times (cm^2/s)$.

amounts adsorbed higher than about 7%. The strong interaction with the penetrating molecules, leading to a high mobility of polymer chains, that can induce structural transformations, as clustering of solvent molecules, crazing or partial dissolution. The systems loose their compactness and diffusion becomes less dependent or even independent of the amount of vapour absorbed as recognizable from the second part of the curves. From the first part of the diffusion curves displayed in Fig. 11, the zero diffusion coefficient, D_0, could be extrapolated for all the samples. At 3 wt% in inorganics (Fig. 12B), only the nanocomposite filled with the PDMS surfactant-treated clay, known to be rather well dispersed in the cured silicone matrix, displays a D_0 value lower than unfilled PDMS. For the other investigated (nano)composites, same or higher values are measured. The horizontal straight line represents the Log D_0 of the unfilled PDMS with respect to n-hexane. Again, the lower recorded D_0 value is found at 3 wt% in inorganics (Fig. 12a) fully confirming the observations previously discussed with acetone vapour.

Using Eqs. (1) and (2) for each n-hexane partial pressure allows obtaining sorption S [cm^3(STP)/(cm^3 atm)] and diffusion D (cm^2/s), their product providing the permeability, as already performed for acetone. Table 4 reports the permeability data to n-hexane vapour pressure in the range of activity 0.2–0.8 for unfilled PDMS and all samples filled with 3 wt% in inorganics. At low activity ($a = 0.2$), the nanocomposite containing the PDMS surfactant-treated clay (i.e., PDMS–3MMT) is characterized by the lower permeability value. However upon increasing the n-hexane vapour pressure, such a behaviour is no longer observed due to the too high affinity of this good solvent for the PDMS chains resulting in very high sorption properties and global permeability behaviour levelling off.

4. Conclusions

Poly(dimethylsiloxane) (PDMS)/clay nanocomposites have been produced using ω-ammonium functionalized oligo-PDMS surfactant (PDMS–N$^+$(CH$_3$)$_3$) and processed in membrane form with different percentages of organoclay (1; 2; 3; 4; 5 and 6 wt%). The clay ion-exchanged by PDMS–N$^+$(CH$_3$)$_3$ has been compared to (nano)compositions prepared with PDMS and either non-exchanged sodium MMT (3 wt%) or two organoclays organo-modified by using non-functional alkyl ammonium cations (C$_{38}$H$_{80}$N$^+$) (3 wt%) or hydroxyalkyl ammonium (C$_{22}$H$_{48}$ON$^+$) cations (3 wt%).

- Morphological analysis conducted by TEM showed that the quality of dispersion of the four different clays was gradually enhanced using compatibilizers promoting attractive interactions with the matrix. The nanocomposites based on PDMS–N$^+$(CH$_3$)$_3$ surfactant exhibited the best degree of dispersion, in particular at 3 wt% of organoclay.
- Viscosity measurements confirmed that an organic surfactant is needed to intercalate the PDMS chains into the clay galleries leading to higher viscosity for all the investigated samples. Comparing the herewith studied organo-modifiers, significantly higher viscosity was observed for the nanocomposites filled with clay modified by PDMS–N$^+$(CH$_3$)$_3$.
- Mechanical properties (Young's Modulus) showed an increasing of stiffness with increasing the content in PDMS-

treated clay, but no significant differences could be detected between the different organo-modifiers.
- Barrier properties (sorption (S), diffusion (D) and permeability ($P = S \cdot D$)) to acetone and n-hexane vapours showed that the sorption is not influenced by the presence of the organo-modified clay, while the diffusion parameter is significantly affected in the range of sorbed vapour 0–4% (g of solvent sorbed/100 g of dry polymer) for acetone and 0–7% for the most interactive n-hexane. The thermodynamic diffusion parameter (D_0) was extrapolated at zero vapour concentration and was compared to the D_0 value of unfilled PDMS. D_0 proved strictly dependent on the morphology of the samples and the quality of the nanoplatelet dispersion throughout the silicone matrix. The lower D_0 value was recorded for the nanocomposition filled with 3 wt% of clay surface-treated by the PDMS–N$^+$(CH$_3$)$_3$ surfactant.

References

[1] Leemann M, Eigenberger G, Strathmann H. J Membr Sci 1996;113(2):313–22.
[2] Stern SA. J Membr Sci 1994;94:1–65.
[3] Exama A, Arul J, Lencki RW, Lee LZ, Toupin C. J Food Sci 1993;58(6):1365–70.
[4] Houston KS, Weinkauf DH, Stewart FF. J Membr Sci 2002;205(1–2):103–12.
[5] Kramer PW, Yeh YS, Yasuda H. J Membr Sci 1989;46(1):1–28.
[6] Cussler EL, Hughes SE, William I, Ward J, Aris R. J Membr Sci 1988;38(2): 161–74.
[7] Gorrasi G, Tortora M, Vittoria V, Pollet E, Lepoittevin B, Alexandre M, et al. Polymer 2003;44(8):2271–9.
[8] Gorrasi G, Tortora M, Vittoria V, Kaempfer D, Mülhaupt R. Polymer 2003;44(13):3679–85.
[9] Demirkol E, Kalyon D. J Appl Polym Sci 2007;104(3):1391–8.
[10] Schmidt D, Clément F, Giannelis E. Adv Funct Mater 2006;16(3):417–25.
[11] Wang J, Chen Y. J Appl Polym Sci 2008;107(4):2059–66.
[12] Ma J, Yu ZZ, Kuan HC, Dasari A, Mai YW. Macromol Rapid Commun 2005;26(10):830–3.
[13] Simon W, Stafford KT, Ou DL. J Inorg Organomet Polym 2008;18(3):364–73.
[14] Lebrun L, Bruzaud S, Grohens Y, Langevin D. Eur Polym J 2006;42(9):1975–85.
[15] Vaugan BR, Marand E. J Membr Sci 2008;310(1–2):197–207.
[16] Liu Q, De Kee D. Can J Chem Eng 2007;85(1):36–44.
[17] Osman M, Atallah A, Müller M, Suter U. Polymer 2001;42(15):6545–56.
[18] Labruyère C, Monteverde F, Alexandre M, Dubois P. J Nanosci Nanotechnol 2009;9(4):2731–8.
[19] Felder RM, Huvard GS. Permeation, diffusion and sorption of gases and vapors. In: Fava RA, editor. Methods of experimental physics. Polymers, physical properties, vol. 16C. New York: Academic Press; 1980. p. 315–77.
[20] Barton AFM. Handbook of polymer–liquid interaction parameters. Boca Raton: Florida: CRC Press; 1990 [section 19]. p. 125–47.
[21] Cassagnau P. Polymer 2008;49(9):2183–96.
[22] Beigbeder A, Linares M, Devalckenaere M, Degée P, Claes M, Beljonne D, et al. Adv Mater 2008;20(5):1003–7.
[23] Sabourault N, Mignani G, Wagner A, Mioskowski C. Org Lett 2002;4(13): 2117–9.
[24] Ray SS, Okamoto M. Prog Polym Sci 2003;28(11):1539–641.
[25] Low H, Liu T, Loh W. Polym Int 2004;53(12):1973–8.
[26] Crank J. The mathematics of diffusion. London: Oxford University Clarendon Press; 1956.
[27] Vieth WR, Amini MA. In: Hopfenberg HB, editor. Permeability of plastic films and coatings. London: Plenum Press; 1974 [chapter 6]. p. 49–61.